On the existence of time delay for rotating beam with proportional–derivative controller

Abstract

A rotating beam at varying speed mathematical model is studied. Multiple time scales method is applied to the nonlinear system of differential equations and investigated the system behavior approximate solution in the instance of resonance case. We studied the system in case of applying the delayed control on the displacement and the velocity with Proportional–derivative (PD) controller. The consistency of the steady state solution in the near-resonance case is reviewed and analyzed using the Routh-Huriwitz approach. The factors on the steady state solution of the various parameters are recognized and discussed. Simulation effects are obtained using MATLAB software package. Different response curves are involved to show and compare controller effects at various system parameters.

1 Introduction

In dynamical and structural structures, disturbances and complex instability are always undesired phenomena. These systems face nonlinear vibrations for numerous purposes, such as materials' nonlinear properties, geometric nonlinearities, and nonlinear powers of excitation. Much time, money and efforts are spent on minimizing these systems' vibrations and oscillations for longer life and preventing them from failure or damage.

Many scholars and scientists have paid attention to and attempted to alleviate this topic that affects equipment, industry, and frugality. The high amplitude nonlinear vibration activity of a revolving cantilever beam is treated by Thomas et al. [1], with applications for turbo machinery and turbo-propeller blades. The effect of rotation speed on the nonlinear vibrations of the beam and particularly on the hardening/softening behaviour of its resonances and the occurrence of high amplitude jump phenomena were investigated. A new dynamic model of a rotating flexible beam with a condensed mass positioned in an arbitrary location, based on the absolute nodal coordinate formulation, was investigated by Zhang et al. [2]. They found that both the magnitude and the direction of the condensed mass impact the normal frequencies and the mode shapes. Aeroelastic analysis of a spinning wind turbine blade was conducted by Rezaei et al.[3] by considering the effects of geometrical nonlinearities associated with large blade deflection created during the operation of the wind turbine. Through applying the concepts of quasi-steady and unsteady airfoil aerodynamics,

they proposed an aerodynamic model based on the strip theory. The results showed that geometrical nonlinearity, especially for larger structural deformations, had a significant impact. The effect of rotation velocity on nonlinear resonances is considered in[4], and the multi-scale perturbation approach is used and solved in the von Kármán[5] model. In order to simulate nonlinear resonances via a one-mode Galerkin expansion, nonlinear beam models such as axial inertia and nonlinear curvature are used. Nonlinear resonance curves are also computed, based on a Galerkin discretization with Legendre polynomials and a continuity process, with a completely numerical approach (harmonic balance coupled to an asymptotic numerical technique). For more detailed and effective dynamic analysis of a rotating cantilever beam with elastic deformation defined by partial integro-differential equations with non-Cartesian deformation variables, Kim and Chung[6] suggested a nonlinear model. They showed that the proposed model not only provided good numerical precision and efficiency, but also overcome the constraints expressed by Cartesian variables of a previous traditional nonlinear model. The dynamics of a structure consisting of a rotating rigid hub and a thin-walled composite beam with an embedded active part were introduced by Latalski [7]. Based on the device rotation velocity and laminae fiber orientation angle, they studied natural mode shapes and electrical field spatial distribution. A Proportional Derivative (PD) controller was applied by Kandil, H. El-Gohary [8] to research the effects of time delay on its output to decrease the oscillations of a spinning beam at different speeds. Although the vibrational modes of the dual system are linearly coupled, the controller is applied to only one mode and the other coupled mode tracks it. In the case of the worst resonance cases that were verified numerically, they regulated the device. Yao et al. [9, 10] applied the theory and isotropic constitutive law of Hamilton in order to infer the beam's governing equations. Of supersonic gas flow and high temperature, they studied the dynamics at different speeds. Choi et al.[11, 12] showed that an active damping effect can be obtained with polyvinylidene fluoride (PVDF) sensors and macrofiber composite (MFC) actuators through a negative velocity feedback control algorithm. MFC is a composite form of piezoelectric material. Through the required arrangement and distribution scale of the sensor/actuator pair, ample vibration suppression efficiency would therefore be obtained.

The system of nonlinear differential equations with and without time delay that describes a rotating beam at varying speeds shown in Figure 1a [8,9, 10] has been studied in this paper in order to reduce its oscillations and enhance its efficiency. The displacements of the blade cross section are measured by using MFC sensors that are distributed over the bottom surface of the blade, as shown in Fig. 1b. The measured signals will be sent back to the computer to analyze and compute the appropriate control signal as shown in Fig. 1c. Once the control signal is calculated, it is passed through conditioning circuit and then be applied to the embedded MFC actuators that are distributed over the top of the blade so that they can modify the blade position and reduce its vibration, a control loop feedback mechanism illustrated in figure 2 are continuously calculates an error value e(t) as the difference between a desired setpoint (SP) and a measured process variable (PV) and applies a correction based on proportional, integral, and derivative terms (denoted P, I, and D respectively).This article is organized as: analytical solutions for the second order nonlinear differential equations that described the system are derived using the multiple time

scales method [5, 13] in Section 2, while a numerical Results and brief discussions are given in Section 3. Finally a brief conclusion is given in Section 4.
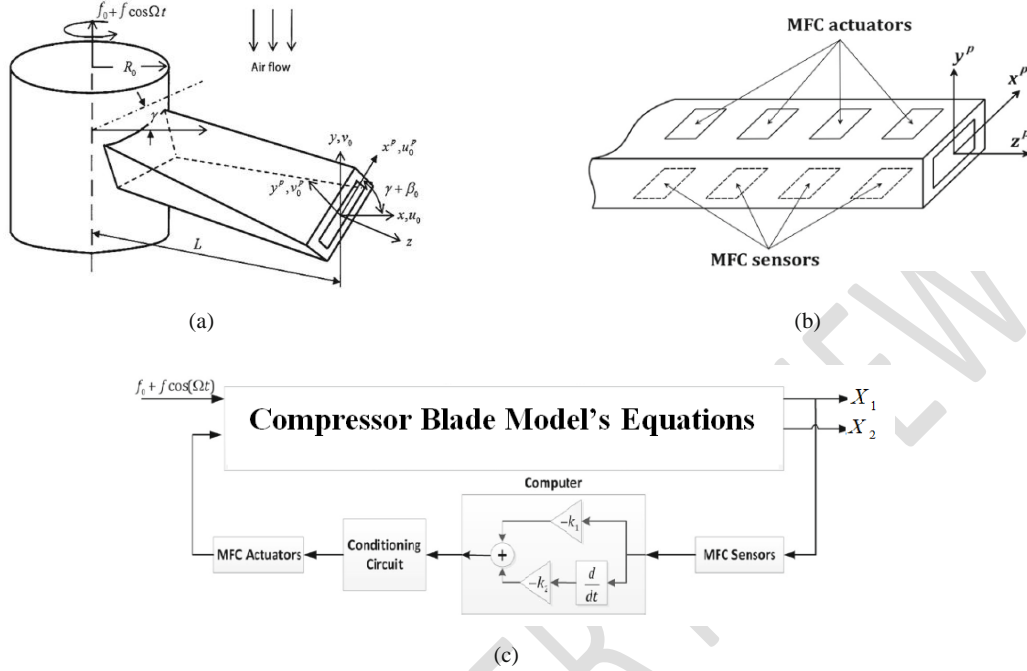

(a)

(b)

(c)

Figure 1 Rotating compressor blade model, (a) thin-walled pre-twisted blade, (b) sensors and actuators distribution and (c) block diagram of control process.
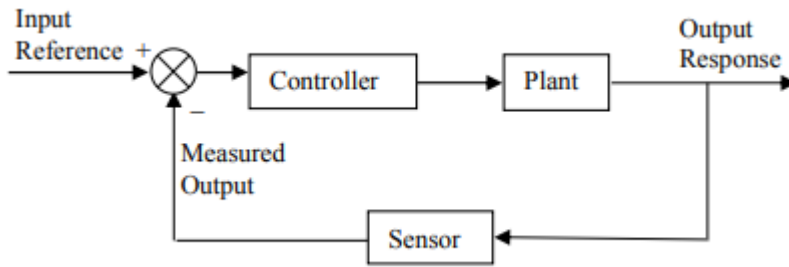

Figure 2 A closed loop system controller.

2 System model and mathematical analysis

The mathematical model for the system shown in figure 1 is given in [5] as:

$$
\begin{aligned}
&\ddot{X}_1 + 2\mu_1 \dot{X}_1 + \omega^2 X_1 + \beta_{13}\dot{X}_2 + \beta_{11}X_2 + \beta_5 X_1 X_2^2 + \beta_5 X_1^3 = 2f_o f\,\beta_{14}X_1\cos(\Omega t)\\
&+ f^2 \beta_{14}X_1\cos^2(\Omega t) + f\,\beta_{16}\Omega\sin(\Omega t) - k_1 X_1(t-\tau) - k_2\dot{X}_1(t-\tau),
\end{aligned}
\tag{1a}
$$

$$
\begin{aligned}
&\ddot{X}_2 + 2\mu_2 \dot{X}_2 + \omega^2 X_2 + \beta_{22}\dot{X}_1 + \beta_{21}X_1 + \beta_5 X_2 X_1^2 + \beta_5 X_2^3 = 2f_o f\,\beta_{24}X_2\cos(\Omega t)\\
&+ f^2 \beta_{24}X_2\cos^2(\Omega t),
\end{aligned}
\tag{1b}
$$

3

where X_1, X_2 are the horizontal and vertical displacements of the blade cross section, μ_1, μ_2 are the damping parameters of the system modes, $\beta_{11}, \beta_{21}, \beta_{13}, \beta_{22}$, are the coupling factors between the system modes, β_5 is the cubic nonlinearity factors between the system modes, β_{14}, β_{24} are the parametric excitation parameters, f_o, f are constant and variable rotating speed, Ω is the excitation frequency, k_1, k_2 are the proportional and derivative feedback gains, and τ is the time delay.

Applying (MTSM) and scaling the previous parameters as:

$$\beta_{11} = \varepsilon\hat{\beta}_{11}, \beta_{13} = \varepsilon\hat{\beta}_{13}, \beta_{14} = \varepsilon\hat{\beta}_{14}, \beta_{16} = \varepsilon\hat{\beta}_{16}, \beta_{21} = \varepsilon\hat{\beta}_{21}, \beta_{22} = \varepsilon\hat{\beta}_{22}, \beta_{24} = \varepsilon\hat{\beta}_{24}, \beta_5 = \varepsilon\hat{\beta}_5,$$
$$k_1 = \varepsilon\hat{k}_1, k_2 = \varepsilon\hat{k}_2, \mu_1 = \varepsilon\hat{\mu}_1, \mu_2 = \varepsilon\hat{\mu}_2. \tag{2}$$

The second order approximation of X_1, X_2 is given by as stated in power series form as:

$$X_1(T_o, T_1, \varepsilon) = X_{10}(T_o, T_1) + \varepsilon X_{11}(T_o, T_1) + O(\varepsilon^2),$$
$$X_2(T_o, T_1, \varepsilon) = X_{20}(T_o, T_1) + \varepsilon X_{21}(T_o, T_1) + O(\varepsilon^2), \tag{3}$$
$$X_1(T_o - \tau, T_1 - \varepsilon\tau, \varepsilon) = X_{10\tau}(T_o, T_1) + \varepsilon X_{11\tau}(T_o, T_1) + O(\varepsilon^2),$$

where the time derivative will takes the values:

$$\frac{d}{dt} = D_0 + \varepsilon D_1 + O(\varepsilon^2), \frac{d^2}{dt^2} = D_o^2 + 2\varepsilon D_0 D_1 + O(\varepsilon^2) \tag{4}$$

and $T_n = \varepsilon^n t$, $D_n = \frac{\partial}{\partial T_n}, n = 0,1$.

Applying equations (2)-(4) into (1) at and equating same power of ε coefficients to obtain:

$$O(\varepsilon^0) : (D_o^2 + \omega^2)X_{10} = 0 \tag{5a}$$

$$(D_o^2 + \omega^2)X_{20} = 0 \tag{5b}$$

$$O(\varepsilon):$$

$$(D_o^2 + \omega^2)X_{11} = \hat{\beta}_{14}f X_{10}\cos(\Omega T_0)[2f_o + f \cos(\Omega T_0)] + f \hat{\beta}_{16}\Omega\sin(\Omega T_0)$$
$$-2D_0 D_1 X_{10} - 2\hat{\mu}_1 D_0 X_{10} - \hat{\beta}_{13}D_0 X_{20} - \hat{\beta}_{11}X_{20} - \hat{\beta}_5 X_{10}X_{20}^2 - \hat{\beta}_5 X_{10}^3 \tag{6a}$$
$$-k_1 X_{10} - k_2 D_0 X_{10} - \hat{k}_1 X_{10\tau} - \hat{k}_2 D_0 X_{10\tau}.$$

$$(D_o^2 + \omega^2)X_{21} = \hat{\beta}_{24}f X_{20}\cos(\Omega T_0)[2f_o + f \cos(\Omega T_0)] - 2D_0 D_1 X_{20} - 2\hat{\mu}_2 D_0 X_{20}$$
$$-\hat{\beta}_{22}D_0 X_{10} - \hat{\beta}_{21}X_{10} - \hat{\beta}_5 X_{20}X_{10}^2 - \hat{\beta}_5 X_{20}^3. \tag{6b}$$

It is well known that solutions of (5a), (5b) are

$$X_{10} = A(T_1)e^{i\omega T_0} + cc.,$$
$$X_{20} = B(T_1)e^{i\omega T_0} + cc., \tag{7}$$
$$X_{10\tau} = A_\tau(T_1)e^{i\omega(T_0 - \tau)} + cc.,$$

Using Taylor expansion, then the value of $A_\tau(T_1)$ is given by $A_\tau(T_1) = A(T_1 - \varepsilon\tau) = A(T_1) - \varepsilon\tau\dot{A}(T_1) + \cdots$. As approximation, we keep only the first term of this expansion, then, $X_{10\tau} = A(T_1)e^{i\omega(T_0-\tau)} + cc.$,

where $cc.$ represents the complex conjugates of the preceding terms and A, B are complex functions of T_1.

Now we will study the system worst operating modes due to resonance cases.

Case 1 Primary resonance:

The primary resonance occur when the value of Ω is equal to ω so we study the behavior of the system near this case i.e.

$$\Omega = \omega + \sigma_1 = \omega + \varepsilon\hat{\sigma}_1, \tag{8}$$

Combining Eq. (7) and (8) into (6) and eliminating all secular terms, we obtain:

$$\frac{\beta_{14}f^2}{2}(A + \bar{A}\frac{e^{2i\sigma_1 t}}{2}) - 2i\,\omega\dot{A} - 2i\,\mu_1\omega A - \beta_{11}B - i\,\omega\beta_{13}B - 2\beta_5 AB\bar{B} - 3\beta_5 A^2\bar{A}$$
$$-\beta_5 B^2\bar{A} - 0.5i\,\beta_{16}\Omega fe^{i\sigma_1 t} - k_1 A\,e^{-i\,\omega\tau} - i\,k_2\omega A\,e^{-i\,\omega\tau} = 0, \tag{9}$$

$$\frac{\beta_{24}f^2}{2}(B + \bar{B}\frac{e^{2i\sigma_1 t}}{2}) - 2i\,\omega\dot{B} - 2i\,\mu_2\omega B - \beta_{21}A - i\,\omega\beta_{22}A - 2\beta_5 AB\bar{A} - 3\beta_5 B^2\bar{B} - \beta_5 A^2\bar{B} = 0 \tag{10}$$

Converting A, B to the polar form then we have:

$$A = \frac{a_1}{2}e^{i\beta_1},$$
$$B = \frac{a_2}{2}e^{i\beta_2} \tag{11}$$

where $a_j, \beta_j, (j = 1, 2)$ are the system amplitude and phase respectively.

Introducing Eq. (11) in Eqn. (9) and (10) and equating the real and imaginary parts we get:

$$\dot{a}_1 = -\mu_1 a_1 - \frac{\beta_{11}a_2}{2\omega}\sin(\varphi_2) - \frac{\beta_{13}a_2}{2}\cos(\varphi_2) + \frac{\beta_5 a_1 a_2^2}{8\omega}\sin(2\varphi_2)$$
$$+ \frac{\beta_{14}a_1 f^2}{8\omega}\sin(2\varphi_1) - \frac{\beta_{16}f\,\Omega}{2\omega}\cos(\varphi_1) + \frac{k_1 a_1}{2\omega}\sin(\omega\tau) - \frac{k_2 a_1}{2}\cos(\omega\tau), \tag{12a}$$

$$\dot{\varphi}_1 = \sigma_1 - \frac{\beta_{11}a_2}{2\omega a_1}\cos(\varphi_2) + \frac{\beta_{13}a_2}{2a_1}\sin(\varphi_2) - \frac{\beta_5 a_2^2}{8\omega}\cos(2\varphi_2) - \frac{\beta_5 a_2^2}{4\omega}$$
$$- \frac{3\beta_5 a_1^2}{8\omega} + \frac{\beta_{14}f^2}{4\omega}(1 + \frac{\cos(2\varphi_1)}{2}) + \frac{\beta_{16}\Omega f}{2\omega a_1}\sin(\varphi_1) - \frac{k_1}{2\omega}\cos(\omega\tau) - \frac{k_2}{2}\sin(\omega\tau), \tag{12b}$$

$$\dot{a}_2 = -\mu_2 a_2 + \frac{\beta_{21}a_1}{2\omega}\sin(\varphi_2) - \frac{\beta_{22}a_1}{2}\cos(\varphi_2) + \frac{\beta_5 a_2 a_1^2}{8\omega}\sin(2\varphi_2)$$
$$- \frac{\beta_{24}a_2 f^2}{8\omega}\sin(2\varphi_2 - 2\varphi_1), \tag{12c}$$

5

$$\dot{\varphi}_2 = \sigma_1 + \frac{\beta_{22} a_1}{2a_2}\sin(\varphi_2) - \frac{\beta_{21} a_1}{2\omega a_2}\cos(\varphi_2) + \frac{\beta_5}{4\omega}(a_1^2 - a_2^2) + \frac{\beta_5}{8\omega}(a_1^2 - a_2^2)\cos(2\varphi_2)$$

$$-\frac{3\beta_5}{8\omega}(a_1^2 - a_2^2) - \frac{\beta_{24} f^2}{8\omega}\cos(2\varphi_2 - 2\varphi_1) + \frac{f^2}{4\omega}(\beta_{14} - \beta_{24}) + \frac{\beta_{13} a_2}{2a_1}\sin(\varphi_2)$$

$$-\frac{\beta_{11} a_2}{2\omega a_1}\cos(\varphi_2) + \frac{\beta_{14} f^2}{8\omega}\cos(2\varphi_1) + \frac{\beta_{16}\Omega f}{2\omega a_1}\sin(\varphi_1) - \frac{k_1}{2\omega}. \tag{12d}$$

Where $\begin{array}{l} \varphi_1 = \sigma_1 t - \beta_1, \\ \varphi_2 = \beta_2 - \beta_1. \end{array}$ (13)

For obtaining the steady state solution for amplitude and phase putting $\dot{a}_1 = \dot{\varphi}_1 = \dot{a}_2 = \dot{\varphi}_2 = 0$ into Eq. (12), the resultant formulas can be solved numerically. To discuss the stability behavior of these solutions, linearizing these equations according to Lyapunov first (indirect) method to give the following system:

$$\begin{bmatrix} \dot{a}_1 \\ \dot{\varphi}_1 \\ \dot{a}_2 \\ \dot{\varphi}_2 \end{bmatrix} = \begin{bmatrix} \dfrac{\partial \dot{a}_1}{\partial a_1} & \dfrac{\partial \dot{a}_1}{\partial \varphi_1} & \dfrac{\partial \dot{a}_1}{\partial a_2} & \dfrac{\partial \dot{a}_1}{\partial \varphi_2} \\[2mm] \dfrac{\partial \dot{\varphi}_1}{\partial a_1} & \dfrac{\partial \dot{\varphi}_1}{\partial \varphi_1} & \dfrac{\partial \dot{\varphi}_1}{\partial a_2} & \dfrac{\partial \dot{\varphi}_1}{\partial \varphi_2} \\[2mm] \dfrac{\partial \dot{a}_2}{\partial a_1} & \dfrac{\partial \dot{a}_2}{\partial \varphi_1} & \dfrac{\partial \dot{a}_2}{\partial a_2} & \dfrac{\partial \dot{a}_2}{\partial \varphi_2} \\[2mm] \dfrac{\partial \dot{\varphi}_2}{\partial a_1} & \dfrac{\partial \dot{\varphi}_2}{\partial \varphi_1} & \dfrac{\partial \dot{\varphi}_2}{\partial a_2} & \dfrac{\partial \dot{\varphi}_2}{\partial \varphi_2} \end{bmatrix} \begin{bmatrix} a_1 \\ \varphi_1 \\ a_2 \\ \varphi_2 \end{bmatrix}$$

$$= \begin{bmatrix} \gamma_{11} & \gamma_{12} & \gamma_{13} & \gamma_{14} \\ \gamma_{21} & \gamma_{22} & \gamma_{23} & \gamma_{24} \\ \gamma_{31} & \gamma_{32} & \gamma_{33} & \gamma_{34} \\ \gamma_{41} & \gamma_{42} & \gamma_{43} & \gamma_{44} \end{bmatrix} \begin{bmatrix} a_1 \\ \varphi_1 \\ a_2 \\ \varphi_2 \end{bmatrix} = [J] \begin{bmatrix} a_1 \\ \varphi_1 \\ a_2 \\ \varphi_2 \end{bmatrix} \tag{14}$$

where the values of $\gamma_{mn}, (m, n = 1, 2, 3, 4)$ are given in "Appendix". Stability of a particular fixed point with respect to perturbation proportional to $\exp(\lambda T_1)$ is determined by zeros of characteristic equation of the jacobian determinate $|J - \lambda I|$ which gives:

$$\lambda^4 + \Pi_1 \lambda^3 + \Pi_2 \lambda^2 + \Pi_3 \lambda + \Pi_4 = 0, \tag{15}$$

where $\Pi_{mn}, m, n = 1:4$ are given in appendix. According to Routh-Hurwitze criteria [17, 18], the necessary and sufficient condition for all characteristic roots of the characteristic equation (15) to have negative real parts if and only if the determinate D and all its principle

minors are positive, where $D = \begin{vmatrix} \Pi_1 & 1 & 0 & 0 \\ \Pi_3 & \Pi_2 & \Pi_1 & 1 \\ 0 & \Pi_4 & \Pi_3 & \Pi_2 \\ 0 & 0 & 0 & \Pi_4 \end{vmatrix}$, then the stability conditions will be

$$\Pi_1 > 0, \ \Pi_4 > 0, \ (\Pi_1\Pi_2 - \Pi_3) > 0, \ [\Pi_3(\Pi_1\Pi_2 - \Pi_3) - \Pi_1^2\Pi_4] > 0, \tag{16}$$

Case 2 Principal parametric resonance

Assume that the detuning parameter σ_2 is to be used to depict the principal parametric resonance as shown in the following relation:

$$\Omega = 2\omega + \sigma_2 = 2\omega + \varepsilon\hat{\sigma}_2 \tag{17}$$

As in case 1 combining Eq. (7) and (17) into (6) and eliminating all secular terms to have:

$$\frac{\beta_{14}f^2}{2}A + \beta_{14}f_o f\ \bar{A}\frac{e^{i\sigma_2 t}}{2} - 2i\,\omega\dot{A} - 2i\,\mu_1\,\omega A - \beta_{11}B - i\,\omega\beta_{13}B \tag{18a}$$

$$-2\beta_5\,A\,B\,\bar{B} - 3\beta_5\,A^2\bar{A} - \beta_5\,B^2\bar{A} - k_1 A\,e^{-i\,\omega\tau} - i\,k_2\,\omega A\,e^{-i\,\omega\tau} = 0,$$

$$\beta_{24}f\,(\frac{Bf}{2} + f_o\,\bar{B}\,e^{i\sigma_2 t}) - 2i\,\omega\dot{B} - 2i\,\mu_2\,\omega B - \beta_{21}A - i\,\omega\beta_{22}A$$

$$-2\beta_5 A\,B\,\bar{A} - 3\beta_5 B^2\bar{B} - \beta_5 A^2\bar{B} = 0 \tag{18b}$$

Using Eq. (11) into (18) and equating the real and imaginary parts to obtain the following system of ordinary differential equations:

$$\dot{a}_1 = -\mu_1 a_1 - \frac{\beta_{11}a_2}{2\omega}\sin(\varphi_2) - \frac{\beta_{13}a_2}{2}\cos(\varphi_2)$$

$$-\frac{\beta_5 a_1 a_2^2}{4\omega}\sin(2\varphi_2) + \frac{\beta_{14}f_o f}{2\omega}\sin(\varphi_1) - \frac{k_1 a_1}{2\omega}\sin(\omega\tau) - \frac{k_2 a_1}{2}\cos(\omega\tau) \tag{19a}$$

$$\dot{\varphi}_1 = \sigma_2 - \frac{\beta_{11}a_2}{\omega a_1}\cos(\varphi_2) + \frac{\beta_{13}a_2}{a_1}\sin(\varphi_2) - \frac{\beta_5 a_2^2}{2\omega}\cos(2\varphi_2)$$

$$-\frac{\beta_5 a_2^2}{2\omega} - \frac{3\beta_5 a_1^2}{4\omega} + \frac{\beta_{14}f}{\omega}(\frac{f}{2} + f_o\cos(\varphi_1)) - \frac{k_1}{\omega}\cos(\omega\tau) - k_2\sin(\omega\tau), \tag{19b}$$

$$\dot{a}_2 = -\mu_2 a_2 + \frac{\beta_{21}a_1}{2\omega}\sin(\varphi_2) - \frac{\beta_{22}a_1}{2}\cos(\varphi_2) + \frac{\beta_5 a_2 a_1^2}{8\omega}\sin(2\varphi_2)$$

$$+\frac{\beta_{24}a_2 f_o f}{2\omega}\sin(\varphi_1 - 2\varphi_2), \tag{19c}$$

$$\dot{\varphi}_2 = \frac{\beta_{22}a_1}{2a_2}\sin(\varphi_2) + \frac{\beta_{21}a_1}{2\omega a_2}\cos(\varphi_2) + \frac{\beta_5 a_1^2}{4\omega}(1 + \frac{\cos(2\varphi_2)}{2}) + \frac{3\beta_5 a_2^2}{8\omega}$$

$$-\frac{\beta_{24}f_o f}{2\omega}\cos(\varphi_1 - 2\varphi_2) + \frac{f^2}{4\omega}\beta_{24} - \frac{\beta_{11}a_2}{2\omega a_1}\cos(\varphi_2) + \frac{\beta_{13}a_2}{2a_1}\sin(\varphi_2)$$

$$-\frac{\beta_5 a_2^2}{4\omega}\cos(2\varphi_2) - \frac{\beta_5 a_2^2}{4\omega} - \frac{3\beta_5 a_1^2}{8\omega} + \frac{\beta_{14}f}{2\omega}(\frac{f}{2} + f_o\cos(\varphi_1)) - \frac{k_1}{2\omega}. \tag{19d}$$

where
$$\begin{aligned}\varphi_1 &= \sigma_2 t - 2\beta_1,\\ \varphi_2 &= \beta_2 - \beta_1.\end{aligned} \tag{20}$$

Similarly For obtaining the steady state solution for amplitude and phase putting $\dot{a}_1 = \dot{\varphi}_1 = \dot{a}_2 = \dot{\varphi}_2 = 0$ into Eq. (19), the resultant formulas can be solved numerically using MATLAB software. To discuss the stability behavior of these solutions, linearizing these equations according to Lyapunov first (indirect) method to give the following system:

$$\begin{bmatrix} \dot{a}_1 \\ \dot{\varphi}_1 \\ \dot{a}_2 \\ \dot{\varphi}_2 \end{bmatrix} = \begin{bmatrix} \zeta_{11} & \zeta_{12} & \zeta_{13} & \zeta_{14} \\ \zeta_{21} & \zeta_{22} & \zeta_{23} & \zeta_{24} \\ \zeta_{31} & \zeta_{32} & \zeta_{33} & \zeta_{34} \\ \zeta_{41} & \zeta_{42} & \zeta_{43} & \zeta_{44} \end{bmatrix} \begin{bmatrix} a_1 \\ \varphi_1 \\ a_2 \\ \varphi_2 \end{bmatrix}$$

(21)

where the values of $\zeta_{mn}, (m, n = 1, 2, 3, 4)$ are given in "Appendix". Numerically, primary resonance is the worst resonance case that is taken into account in the discussions.

3 Results and discussion

In this section we illustrate the behavior of the system amplitude and phase at various resonance cases. We will show a comparison between active and time delay control and the effect of some system parameters on its amplitude.

3.1 time history

Figure3 (a, b) shows the time response for the amplitude X_1, X_2, where figure 3 (c) illustrates the system phase plane,

Without resonance case and without applying any control system (i.e. $k_1 = k_2 = 0$) at the following parameter variables:

$\omega = 65, \Omega = 100, \mu_1 = \mu_2 = 0.5, \beta_{11} = -0.003, \beta_{13} = -0.82, \beta_{14} = 0.55, \beta_{16} = 6.55,$
$\beta_5 = 0.9, \beta_{22} = -0.82, \beta_{21} = -0.001, \beta_{24} = 0.5, f_o = 7, f = 2, \tau = 0.$
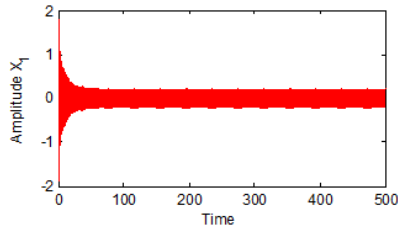
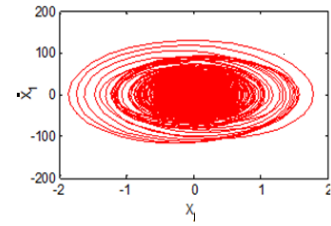| Fig. 3 (a) the time response for the amplitude X_1. | Fig. 3 (b) the time response for the amplitude X_2. | Fig. 3 (c) system phase plane |
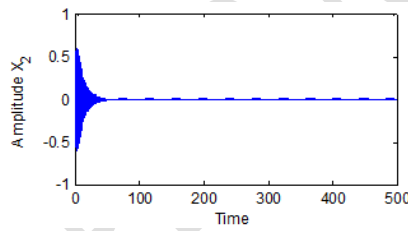
Figure 4 also shows the Time history without control and with primary resonance at the same previous parameters except that $\Omega = \omega = 99$ we observe that the amplitude and the phase are increased due to the resonance operating point.
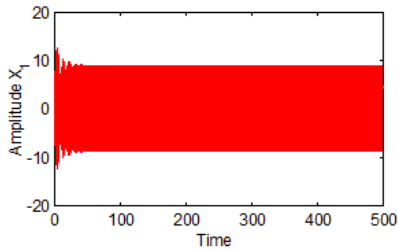

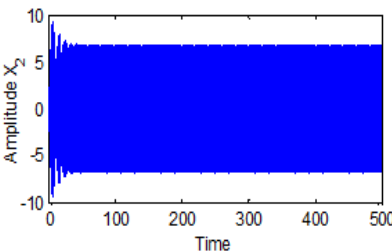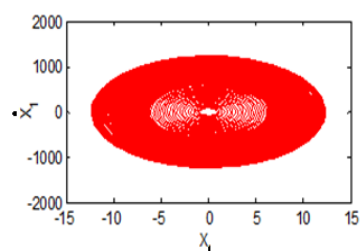| Fig. 4 (a) the time response for the Amplitude X_1. | Fig. 4 (b) the time response for the amplitude X_2 | Fig. 4 (c) system phase plane |

Now applying active and time delay control for the system with primary resonance and comparing the amplitudes. Figure 5, 6 shows the effect of active and time delay control on both X_1, X_2. We observe that the effective of active control is about 105%, and Time delay controller is about 125% so the time delay controller is more efficient than active velocity feed-back controller for this system.
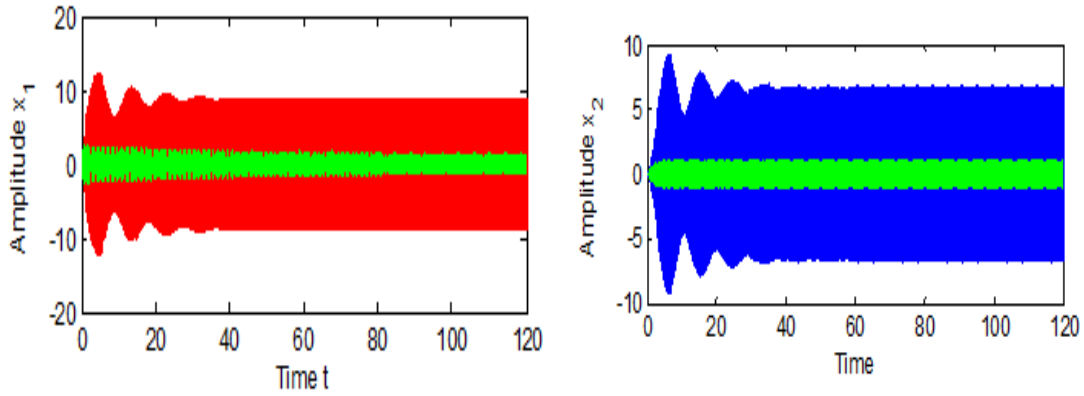
Figure 5 (a, b) effect of active control on x_1, x_2 respectively at primary resonance case.
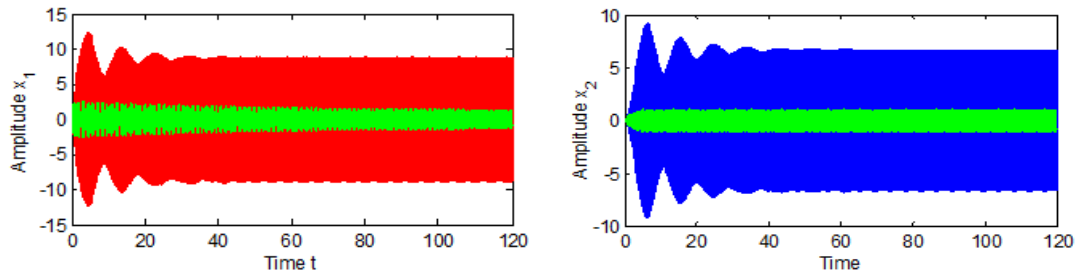

Figure 6 (a, b) effect of time delay control on x_1, x_2 respectively at primary resonance case, $\tau = 0.0015$.

3.2 comparisons with numerical method

In this sub-section we compare the amplitude induced by analytic method (MTSM) and numerical method using Rung-Kutta Method (RKM). In figure 7 system modes amplitudes are plotted with time in both cases analytic and numerical method using the same parameter values in sub-section 3.1 for figure 4, but figure 8 is plotted for $\tau = 0.0015$.
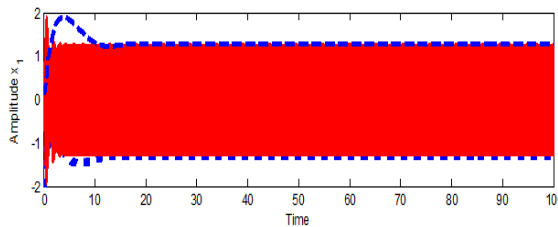
Fig. 7 (a) Time history for the amplitude X_1 using MTSM (blue curve) and RKM (red curve).
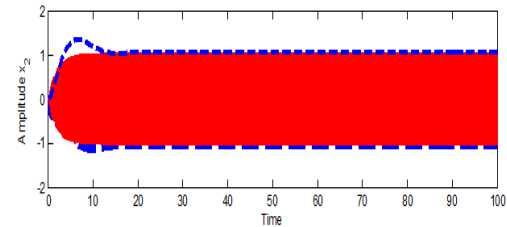
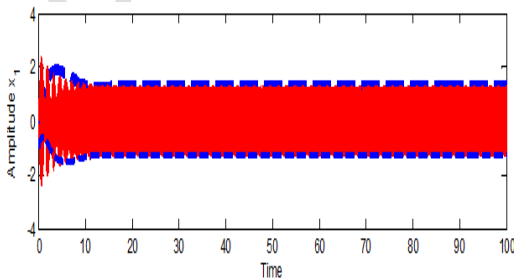Fig. 7 (b) Time history for the amplitude X_2 using RKM (blue curve) and MTSM (red curve).

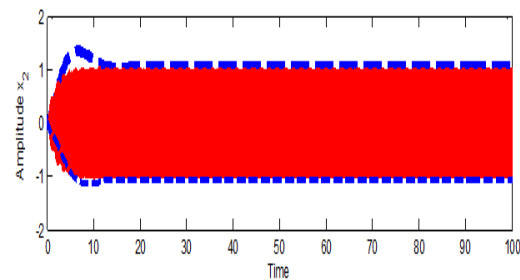Fig. 8 (a) Time history for the amplitude X_1 using MTSM (blue curve) and RKM (red curve) for $\tau = 0.0015$.

Fig. 8 (b) Time history for the amplitude X_2 using MTSM (blue curve) and RKM(red curve) for $\tau = 0.0015$.

3.3 Frequency response

9

Now the following figures show the system amplitude against the detuning parameter σ_1 with change in specified values for system parameters. In figure 9 the parameters a_1, a_2 with σ_1, in case of primary resonance case with:

$$\omega = \Omega = 100, \ \mu_1 = 0.9, \mu_2 = 0.7, \ \beta_{11} = -0.003, \ \beta_{13} = -0.82, \ \beta_{14} = 0.55, \beta_{16} = 6.55, \beta_5 = 0.9,$$

$$\beta_{22} = -0.82, \ \beta_{21} = -0.001, \ \beta_{24} = 0.5, f_o = 7, f = 3, \ \tau = 0.0015, \varepsilon = 0.001 \ , \ k_1 = 1000, k_2 = 0.7, 1, 1.5$$

we observe that the amplitude decreases with the increase of the gain k_2. Figure 10, 11 illustrates the effect of σ_1 on the amplitude with various values of the damping parameter μ_1, μ_2 as given in the figures respectively. The same system parameters values as given for figure9 are used and $k_2 = 1$. We observe in fig. 10that the values of a_1, a_2 are proportional inversely with the damping parameter μ_1 but in fig. 11 the value of a_1 is approximately constant with μ_2 as it is effect on the velocity $\dot{X}_2$ of the system second mode.

3.4Amplitude vs. certain system parameters

Let us consider the parameters given in sub-section 3.3 unless otherwise specified.In this sub-section weshows the change of amplitude range with varying of the constant and variable rotating forces f_o, f as shown in figure 12 (a, b) respectively, $\Omega = 90, \omega = 15, k_2 = 100$. The steady state amplitude of the main system is a monotonic increasing function of the excitation amplitude up to maximum amplitude at saturation. The saturation value may lead to an unstable or damaged system due to its large value. Figure 13 (a, b) describe the behavior of the amplitude with damping parameters μ_1, μ_2 respectivelyat $\Omega = \omega = 10$.
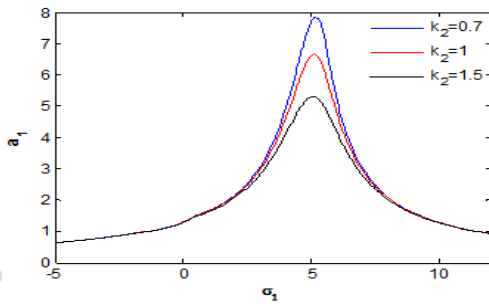

Fig. 9 (a) System amplitude a_1 against detuning parameter σ_1 at $k_2 = 0.7, 1, 1.5$.
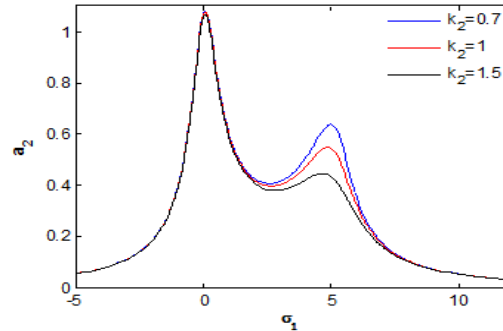
Fig. 9 (b) System amplitude a_2 against detuning parameter σ_1 at $k_2 = 0.7, 1, 1.5$.
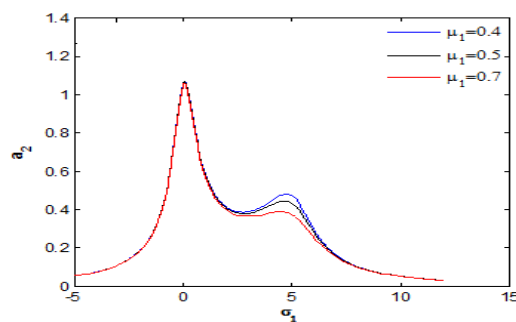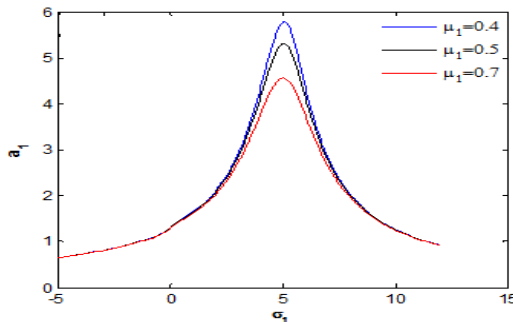
Fig. 10 (a) System amplitude a_1 against detuning parameter σ_1 at $\mu_1 = 0.4,\ 0.5,\ 0.7$.

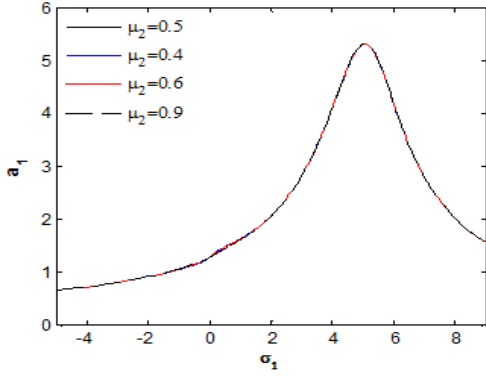Fig. 10 (b) System amplitude a_2 against detuning parameter σ_1 at $\mu_1 = 0.4,\ 0.5,\ 0.7$.

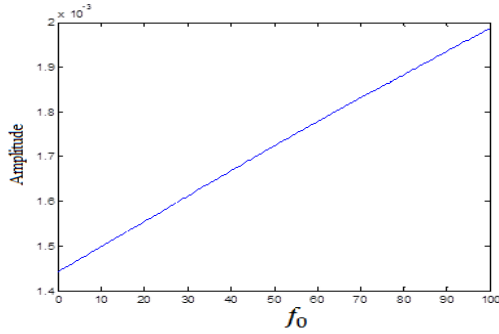Fig. 11 (a) System amplitude a_1 against detuning parameter σ_1 at $\mu_2 = 0.4,\ 0.5,\ 0.6, 0.9$.
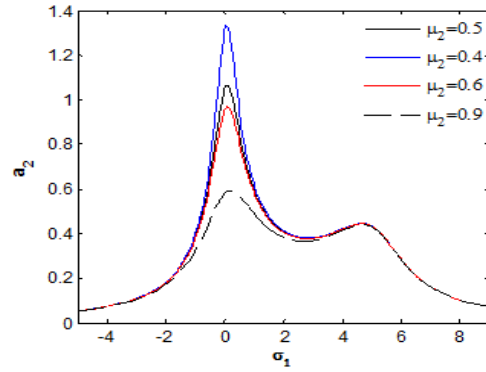
Fig. 11 (b) System amplitude a_2 against detuning parameter σ_1 at $\mu_2 = 0.4,\ 0.5,\ 0.6, 0.9$.

Fig. 12 (a) System amplitude against constant rotating forces f_o
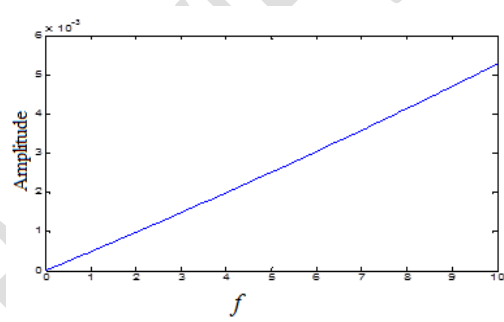
Fig. 12 (b) System amplitude against variable rotating forces f
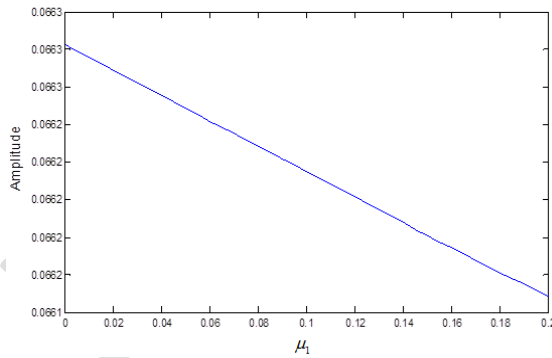
Fig. 13 (a) System amplitude against damping parameters μ_1
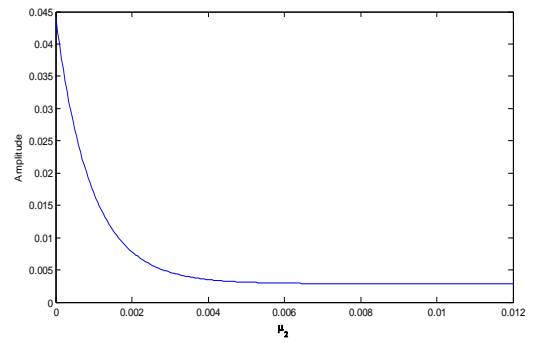
Fig. 13 (b) System amplitude against damping parameters μ_2

4 Conclusions

In this research, a system of nonlinear ordinary differential equations that describing a rotating beam was analyzed analytically via multiple time scales method. We were studied the existence and nonexistence of the time delay effect on the system amplitude in case of the worst resonance cases that were primary resonance and principal parametric resonance. We concluded that the time delay controller is more efficient than active velocity feed-back controller for this system, as the effective of active control is about 105%, and Time delay controller is about 125%. In addition, analytic solutions were compared with numerical

11

approximation solutions using Rung-Kutta method. The effects of parameters on the system amplitude were discussed.

Appendix

$$\gamma_{11} = -\mu_1 - \frac{\beta_5 a_2^2 \sin(2\varphi_2)}{8\omega} + \frac{\beta_{14} f^2 \sin(2\varphi_1)}{8\omega} - \frac{k_2}{2},$$

$$\gamma_{12} = \frac{\beta_{14} f^2 a_1 \cos(2\varphi_1)}{4\omega} + \frac{\beta_{16} \Omega f \sin(\varphi_1)}{2\omega},$$

$$\gamma_{13} = -\frac{\beta_{13} \cos(\varphi_2)}{2} - \frac{\beta_{11} \sin(\varphi_2)}{2\omega} - \frac{\beta_5 a_1 a_2 \sin(2\varphi_2)}{4\omega},$$

$$\gamma_{14} = \frac{\beta_{13} a_2 \sin(\varphi_2)}{2} - \frac{\beta_{11} a_2 \cos(\varphi_2)}{2\omega} - \frac{\beta_5 a_1 a_2^2 \cos(2\varphi_2)}{4\omega},$$

$$\gamma_{21} = -\frac{\beta_{13} a_2 \sin(\varphi_2)}{2a_1^2} + \frac{\beta_{11} a_2 \cos(\varphi_2)}{2\omega a_1^2} - \frac{3\beta_5 a_1}{4\omega} - \frac{\beta_{16} \Omega f \sin(\varphi_1)}{2\omega a_1^2},$$

$$\gamma_{22} = -\frac{\beta_{14} f^2 \sin(2\varphi_1)}{4\omega} + \frac{\beta_{16} \Omega f \cos(\varphi_1)}{2\omega a_1},$$

$$\gamma_{23} = \frac{\beta_{13} \sin(\varphi_2)}{2a_1} - \frac{\beta_{11} \cos(\varphi_2)}{2\omega a_1} - \frac{\beta_5 a_2}{2\omega} - \frac{\beta_5 a_2 \cos(2\varphi_2)}{4\omega},$$

$$\gamma_{24} = \frac{\beta_{13} a_2 \cos(\varphi_2)}{2a_1} + \frac{\beta_{11} a_2 \sin(\varphi_2)}{2\omega a_1} + \frac{\beta_5 a_2^2 \sin(2\varphi_2)}{4\omega},$$

$$\gamma_{31} = -\frac{\beta_{22} \cos(\varphi_2)}{2} + \frac{\beta_{21} \sin(\varphi_2)}{2\omega} + \frac{\beta_5 a_1 a_2 \sin(2\varphi_2)}{4\omega},$$

$$\gamma_{32} = \frac{\beta_{24} f^2 a_2 \cos(2\varphi_2 - 2\varphi_1)}{4\omega},$$

$$\gamma_{33} = -\mu_2 + \frac{\beta_5 a_1^2 \sin(2\varphi_2)}{8\omega} - \frac{\beta_{24} f^2 \sin(2\varphi_2 - 2\varphi_1)}{8\omega},$$

$$\gamma_{34} = \frac{\beta_{22} a_1 \sin(\varphi_2)}{2} + \frac{\beta_{21} a_1 \cos(\varphi_2)}{2\omega} + \frac{\beta_5 a_1^2 a_2 \cos(2\varphi_2)}{4\omega} - \frac{\beta_{24} f^2 a_2 \cos(2\varphi_2 - 2\varphi_1)}{4\omega},$$

$$\gamma_{41} = \frac{\beta_{22} \sin(\varphi_2)}{2a_2} + \frac{\beta_{21} \cos(\varphi_2)}{2\omega a_2} + \frac{\beta_5 a_1}{2\omega}(\frac{\cos(2\varphi_2)}{2} - \frac{1}{2}) - \frac{\beta_{13} a_2 \sin(\varphi_2)}{2a_1^2}$$
$$+ \frac{\beta_{11} a_2 \cos(\varphi_2)}{2\omega a_1^2} - \frac{\beta_{16} \Omega f \sin(\varphi_1)}{2\omega a_1^2},$$

$$\gamma_{42} = \frac{\beta_{24} f^2 \sin(2\varphi_1 - 2\varphi_2)}{4\omega} - \frac{\beta_{14} f^2 \cos(2\varphi_1)}{4\omega} + \frac{\beta_{16} \Omega f \cos(\varphi_1)}{2\omega a_1},$$

$$\gamma_{43} = -\frac{\beta_{22} a_1 \sin(\varphi_2)}{2a_2^2} - \frac{\beta_{21} a_1 \cos(\varphi_2)}{2\omega a_2^2} + \frac{\beta_5 a_2}{2\omega}(\frac{\cos(2\varphi_2)}{2} + \frac{1}{2}) + \frac{\beta_{13} \sin(\varphi_2)}{2a_1} - \frac{\beta_{11} \cos(\varphi_2)}{2\omega a_1},$$

$$\gamma_{44} = \frac{\beta_{22} a_1 \cos(\varphi_2)}{2a_2} - \frac{\beta_{21} a_1 \sin(\varphi_2)}{2\omega a_2} + \frac{\beta_5 \sin(2\varphi_2)}{4\omega}(a_2^2 - a_1^2) - \frac{\beta_{24} f^2 \sin(2\varphi_1 - 2\varphi_2)}{4\omega}$$

$$+ \frac{\beta_{13} a_2 \cos(\varphi_2)}{2 a_1} + \frac{\beta_{11} a_2 \sin(\varphi_2)}{2\omega a_1},$$

$$\zeta_{11} = -\mu_1 - \frac{\beta_5 a_2^2 \sin(2\varphi_2)}{8\omega} + \frac{\beta_{14} f_o f \sin(\varphi_1)}{2\omega} - \frac{k_2}{2},$$

$$\zeta_{12} = \frac{\beta_{14} f_o f a_1 \cos(\varphi_1)}{2\omega},$$

$$\zeta_{13} = -\frac{\beta_{13} \cos(\varphi_2)}{2} - \frac{\beta_{11} \sin(\varphi_2)}{2\omega} - \frac{\beta_5 a_1 a_2 \sin(2\varphi_2)}{4\omega},$$

$$\zeta_{14} = \frac{\beta_{13} a_2 \sin(\varphi_2)}{2} - \frac{\beta_{11} a_2 \cos(\varphi_2)}{2\omega} - \frac{\beta_5 a_1 a_2^2 \cos(2\varphi_2)}{4\omega},$$

$$\zeta_{21} = -\frac{\beta_{13} a_2 \sin(\varphi_2)}{a_1^2} + \frac{\beta_{11} a_2 \cos(\varphi_2)}{\omega a_1^2} - \frac{3\beta_5 a_1}{2\omega},$$

$$\zeta_{22} = -\frac{\beta_{14} f_o f \sin(\varphi_1)}{\omega},$$

$$\zeta_{23} = \frac{\beta_{13} \sin(\varphi_2)}{a_1} - \frac{\beta_{11} \cos(\varphi_2)}{\omega a_1} - \frac{\beta_5 a_2}{\omega} - \frac{\beta_5 a_2 \cos(2\varphi_2)}{2\omega},$$

$$\zeta_{24} = \frac{\beta_{13} a_2 \cos(\varphi_2)}{a_1} + \frac{\beta_{11} a_2 \sin(\varphi_2)}{\omega a_1} + \frac{\beta_5 a_2^2 \sin(2\varphi_2)}{2\omega},$$

$$\zeta_{31} = -\frac{\beta_{22} \cos(\varphi_2)}{2} + \frac{\beta_{21} \sin(\varphi_2)}{2\omega} + \frac{\beta_5 a_1 a_2 \sin(2\varphi_2)}{4\omega},$$

$$\zeta_{32} = \frac{\beta_{24} f_o f a_2 \cos(2\varphi_2 - \varphi_1)}{2\omega},$$

$$\zeta_{33} = -\mu_2 + \frac{\beta_5 a_1^2 \sin(2\varphi_2)}{8\omega} + \frac{\beta_{24} f_o f \sin(2\varphi_2 - \varphi_1)}{2\omega},$$

$$\zeta_{34} = \frac{\beta_{22} a_1 \sin(\varphi_2)}{2} + \frac{\beta_{21} a_1 \cos(\varphi_2)}{2\omega} + \frac{\beta_5 a_1^2 a_2 \cos(2\varphi_2)}{4\omega} - \frac{\beta_{24} f_o f a_2 \cos(2\varphi_2 - \varphi_1)}{\omega},$$

$$\zeta_{41} = \frac{\beta_{22}\sin(\varphi_2)}{2a_2} + \frac{\beta_{21}\cos(\varphi_2)}{2\omega a_2} + \frac{\beta_5 a_1}{2\omega}\left(\frac{\cos(2\varphi_2)}{2} - \frac{1}{2}\right) - \frac{\beta_{13} a_2 \sin(\varphi_2)}{2a_1^2} + \frac{\beta_{11} a_2 \cos(\varphi_2)}{2\omega a_1^2},$$

$$\zeta_{42} = -\frac{\beta_{24} f_o f \sin(2\varphi_2 - \varphi_1)}{2\omega} - \frac{\beta_{14} f_o f \sin(\varphi_1)}{2\omega},$$

$$\zeta_{43} = -\frac{\beta_{22} a_1 \sin(\varphi_2)}{2a_2^2} - \frac{\beta_{21} a_1 \cos(\varphi_2)}{2\omega a_2^2} + \frac{\beta_5 a_2}{2\omega}\left(\frac{1}{2} - \frac{\cos(2\varphi_2)}{2}\right) + \frac{\beta_{13}\sin(\varphi_2)}{2a_1} - \frac{\beta_{11}\cos(\varphi_2)}{2\omega a_1},$$

$$\zeta_{44} = \frac{\beta_{22} a_1 \cos(\varphi_2)}{2a_2} - \frac{\beta_{21} a_1 \sin(\varphi_2)}{2\omega a_2} + \frac{\beta_5 \sin(2\varphi_2)}{4\omega}(a_2^2 - a_1^2) + \frac{\beta_{24} f_o f \sin(2\varphi_2 - \varphi_1)}{4\omega}$$
$$+ \frac{\beta_{13} a_2 \cos(\varphi_2)}{2a_1} + \frac{\beta_{11} a_2 \sin(\varphi_2)}{2\omega a_1},$$

$$\Pi_1 = -(\gamma_{11} + \gamma_{22} + \gamma_{33} + \gamma_{44}),$$

$$\Pi_2 = \gamma_{11}\gamma_{22} + \gamma_{33}\gamma_{44} + (\gamma_{11} + \gamma_{22})(\gamma_{33} + \gamma_{44})$$
$$- [\gamma_{12}\gamma_{21} + \gamma_{13}\gamma_{31} + \gamma_{14}\gamma_{41} + \gamma_{23}\gamma_{32} + \gamma_{24}\gamma_{42} + \gamma_{34}\gamma_{43}],$$

$$\Pi_3 = -\gamma_{11}[\gamma_{22}(\gamma_{33} + \gamma_{44}) - \gamma_{43} + \gamma_{33}\gamma_{44} - \gamma_{23}\gamma_{32} - \gamma_{24}\gamma_{42}] - \gamma_{22}(\gamma_{33}\gamma_{44} - \gamma_{34}\gamma_{43})$$
$$- \gamma_{23}(\gamma_{34}\gamma_{42} - \gamma_{32}\gamma_{44}) - \gamma_{24}(\gamma_{32}\gamma_{43} - \gamma_{22}\gamma_{33}) + \gamma_{12}[\gamma_{21}(\gamma_{33} + \gamma_{44}) - \gamma_{23}\gamma_{31} + \gamma_{24}\gamma_{41}]$$
$$+ \gamma_{13}[\gamma_{31}(\gamma_{22} + \gamma_{44}) - \gamma_{32}\gamma_{21} - \gamma_{34}\gamma_{41}] + \gamma_{14}[\gamma_{41}(\gamma_{22} + \gamma_{33}) - \gamma_{42}\gamma_{21} - \gamma_{43}\gamma_{31}],$$

$$\Pi_4 = -\Pi_1 + \gamma_{11}[\gamma_{23}(\gamma_{34}\gamma_{42} - \gamma_{32}\gamma_{44}) + \gamma_{24}(\gamma_{43}\gamma_{32} - \gamma_{33}\gamma_{42}) - \gamma_{34}\gamma_{43}]$$
$$+ \gamma_{21}\gamma_{12}(\gamma_{34}\gamma_{43} - \gamma_{33}\gamma_{44}) + \gamma_{12}\gamma_{23}(\gamma_{31}\gamma_{44} - \gamma_{34}\gamma_{41}) - \gamma_{12}\gamma_{24}(\gamma_{31}\gamma_{43} - \gamma_{33}\gamma_{41})$$
$$+ \gamma_{13}[\gamma_{21}(\gamma_{32}\gamma_{44} - \gamma_{34}\gamma_{42}) + \gamma_{22}(\gamma_{34}\gamma_{41} - \gamma_{31}\gamma_{44}) + \gamma_{24}(\gamma_{31}\gamma_{42} - \gamma_{32}\gamma_{41})]$$
$$+ \gamma_{14}[\gamma_{21}(\gamma_{33}\gamma_{42} - \gamma_{32}\gamma_{43}) + \gamma_{22}(\gamma_{31}\gamma_{43} - \gamma_{41}\gamma_{33}) + \gamma_{14}(\gamma_{41}\gamma_{32} - \gamma_{42}\gamma_{31})].$$

References

[1] Thomas, O., Sénéchal, A., Deü, J.-F.: Hardening/softening behavior and reduced ordermodeling of nonlinear vibrationsof rotating cantilever beams. Nonlinear Dyn. **86**, 1293–1318(2016).

[2] Zhang, X., Zhang, D., Chen, S., Hong, J.: Modal characteristics of a rotating flexible beam with a concentrated massbased on the absolute nodal coordinate formulation. NonlinearDyn. **88**, 61–77 (2017)

[3] Rezaei, M.M., Behzad, M., Haddadpour, H., Moradi, H.: Aeroelastic analysis of a rotating wind turbine blade using ageometrically exact formulation. Nonlinear Dyn. **89**, 2367– 2392 (2017).

[4] Arvin, H., Bakhtiari-Nejad, F.: Non-linear modal analysis ofa rotating beam. Int. J. Non-Linear Mech. **46**(6), 877–897(2011).

[5] Bekhoucha, F., Rechak, S., Duigou, L., Cadou, J.-M.: Nonlinear forced vibrations of rotating anisotropic beams. NonlinearDyn. **74**(4), 1281–1296 (2013).

[6] Kim, H., Chung, J.: Nonlinear modeling for dynamic analysis of a rotating cantilever beam, Nonlinear Dyn. **86**, 1981–2002 (2016).

[7] Latalski, J.: A coupled-field model of a rotating composite beam with an integrated nonlinear piezoelectric activeelement. Nonlinear Dyn. **90**, 2145–2162 (2017).

[8] Ali Kandil, Hany El-Gohary, Investigating the performance of a time delayed proportional derivative controller for rotating bladevibrations, Nonlinear Dyn 91:2631–2649 (2018).

[9] Yao, M.H., Chen, Y.P., Zhang, W.: Nonlinear vibrations of blade with varying rotating speed, Nonlinear Dyn. **68**, 487–504 (2012).

[10] Yao, M.H., Zhang, W., Chen, Y.P.: Analysis on nonlinear oscillations and resonant responses of a compressor blade,Acta Mech.,**225**, 3483–3510 (2014).

[11] Choi, S.C., Park, J.S., Kim, J.H.: Active damping of rotating composite thin-walled beams using

MFC actuators and PVDF sensors, Compos. Struct.,**76**, 362–374 (2006).

[12] Choi, S.C., Park, J.S., Kim, J.H.: Vibration control of pre-twisted rotating composite thin-walled beams with piezoelectricfiber composites, J. Sound Vib. **300**, 176–196(2007).

[13] Nayfeh, A.H., Mook, D.T.: Nonlinear Oscillations. Wiley,New York (1995).

[14] Katsuhiko, O., System Dynamics (4th ed.), University of Minnesota, p. 617 (2005).

[15] Farhan A. Salem, Ayman A. Aly, PD Controller Structures: Comparison and Selection for an Electromechanical System, Int. Sys. and Appl. Journal, 02, 1-12, 2015.

[16] Richard C.Dorf, Robert H.Bishop, Modern Control Systems, Twelfth Edition, Pearson (2010).

[17] I. S. Gradshteyn and L. M. Ryzhik, 6th Ed. San Diego, Ca: Academic Press, 2000, pp. 1076.

[18] Robert L. Borrelli, Courtney S. Colman, Differential Equation, John Wiley& Sons, INC., New York, 1998.